CE by: SDB UK English FDR428608 on 2 May 2012

IOP PUBLISHING FLUID DYNAMICS RESEARCH

Fluid Dyn. Res. **14** (2012) 000000 (21pp) UNCORRECTED PROOF

Travelling waves in axisymmetric pipe flows

Francesco Fedele

School of Civil and Environmental Engineering, School of Electrical and Computer Engineering, Georgia Institute of Technology, Atlanta, GA, USA

E-mail: fedele@gatech.edu

Received 21 April 2011, in final form 18 March 2012
Published xxx
Online at stacks.iop.org/FDR/14/000000

Communicated by E Knobloch

Abstract
The weakly nonlinear dynamics of axisymmetric Poiseuille pipe flows is investigated. It is shown that small perturbations of the laminar flow with amplitude $\epsilon \sim O(Re^{-2.5})$ obey a coupled system of nonlinear Korteweg–de Vries-type equations. To leading order, these support inviscid soliton-type solutions and periodic waves in the form of toroidal vortex tubes that, due to viscous effects, slowly decay in time on a longer time scale $t \sim O(\epsilon^{-2.5})$, irrespective of higher-order nonlinearities. Q1

1. Introduction

The laminar Hagen–Poiseuille flow is believed to be linearly stable to periodic or localized infinitesimal disturbances for all Reynolds numbers Re (see, e.g., Drazin and Reid (1981)), unlike rotating pipe flows that exhibit a classic supercritical bifurcation (Mackrodt 1976). This indicates that in non-rotating pipe flows, nonlinearities play a particularly important role in shaping the dominant structures at transition, which is triggered by finite-amplitude perturbations (Hof *et al* 2003). In experiments, at a critical fluid speed an intermittent turbulent region develops along the pipe dominated by localized patches, known as puffs, and slug structures (Wygnanski and Champagne 1973, Wygnanski *et al* 1975). They arise as a result of non-axisymmetric perturbations, although strong axisymmetric input can lead to similar turbulent structures (Leite 1959, Fox *et al* 1968). Slugs extend in the streamwise direction filling the entire cross-section of the pipe, especially near the wall, whereas puffs are concentrated near the pipe axis and are surrounded upstream and downstream by laminar flow. Self-sustained turbulence is observed at $Re \approx 2000$, and at $Re \approx 2250$ puffs appear, which as Re increases slowly delocalize by splitting into two or more puffs, eventually expanding into slug flow.

To explain such phenomena, Schmid and Henningson (2001) have suggested that transition occurs due to transient algebraic energy growth of linear disturbances, due to the non-normality of the linearized Navier–Stokes operator. Recently, Pringle and Kerswell (2010) extended such a concept to nonlinear disturbances. Other recent studies try

0169-5983/12/000000+21$33.00

to explain transition in terms of exact nonlinear solutions to the Navier–Stokes equations in the form of steady or travelling waves and periodic patterns (Waleffe 1995a,b, 1997, Faisst and Eckhardt 2003, Wedin and Kerswell 2004, Kerswell 2005, Kerswell and Tutty 2007, Gibson *et al* 2008, Willis *et al* 2008, Willis and Kerswell 2009). Their dominant feature is the nonlinear interaction of streamwise vortices and streaks of the self-sustaining processes formulated by Waleffe (1995a,b, 1997). A recent experimental work by Hof *et al* (2004) has provided physical evidence that such special patterns can occur in turbulent pipe flows. Their relevance to the understanding of turbulence is twofold. First, they seem to share the same mean properties as the turbulent flow. On the other hand, they are believed to form the skeleton of the turbulent attractor that separates from the laminar state through a chaotic edge or boundary of turbulence (Schneider *et al* 2007, Duguet 2008, Duguet *et al* 2008, Willis and Kerswell 2008). Indeed, if the Navier–Stokes equations are viewed as a dynamical system, self-sustaining states correspond to saddle points in an infinite-dimensional phase space. They form a rigid web of heteroclinic connections through their stable and unstable manifolds that organize the turbulent dynamics. Recent numerical studies in turbulent pipe flows (Wedin and Kerswell 2004, Kerswell 2005, Kerswell and Tutty 2007) as well as in Couette flows (Gibson *et al* 2008) provide evidence that turbulence can be understood as an effective random walk in phase space, where turbulent trajectories visit the neighbourhoods of equilibria, travelling waves or periodic orbits, switching from one saddle to the other through their stable and unstable manifolds (Cvitanović and Eckhardt 1991, Cvitanović 1995).

On the other hand, non-rotating axisymmetric pipe flows do not exibhit chaotic or turbulent behaviour. Currently, numerical simulations seem to suggest that such flows are nonlinearly stable (see, e.g., Patera and Orszag 1981, Willis and Kerswell 2008). Theoretical investigations which attempted to prove or disprove this assertion have been limited by the challenge of studying small flow perturbations bifurcating from infinity. Unfortunately, weakly nonlinear approaches may not be appropriate for such an analysis (see Rosenblat and Davis 1979). In fact, Davey and Nguyen (1971) predicted that nonlinearity increases the damping rate of a disturbance of small but finite amplitude localized near the axis of the pipe, whereas Itoh (1977) for the same centre mode found the opposite result. Both their methods are theoretically sound, but as pointed out by Rosenblat and Davis (1979) the authors have constructed amplitude equations for the small-norm bifurcation solution with a dominant structure as that of the least stable linear eigenmode. However, bifurcation from infinity occurs as a result of a strongly nonlinear balance between viscous and inertial effects, and thus it is not a weakly nonlinear phenomenon, even though it is concerned with small-norm solutions. Q2 As pointed out by Davey (1977), calculations to higher order for determining more terms in the amplitude equation would be needed to correctly predict subcritical instability, if any occurs.

For non-rotating non-axisymmetric pipe flows, Smith and Bodonyi (1982) found nonlinear neutral centre modes, hereafter labelled as SB modes, in the form of inviscid travelling waves of small but finite amplitude, which are unstable equilibrium states (see Walton 2004). More recently, Walton (2011) studied the nonlinear stability of impulsively started pipe flows to axisymmetric disturbances at high Reynolds numbers and found the axisymmetric analogue of SB modes, also primarily governed by inviscid dynamics. Walton's neutral mode and the inviscid axisymmetric 'slug' structure proposed by Smith *et al* (1990) are similar to the slugs of vorticity that have been observed in both experiments (Wygnanski and Champagne 1973) and numerical simulations (Willis and Kerswell 2009). As pointed out by Walton (2011), it would be a bit of a stretch to suggest that these neutral modes are the same as the experimental slugs; however, such inviscid structures may play a role in pipe flow transition as precursors to puffs and slugs, since most likely they represent unstable equilibrium states, as do the SB modes (see Walton 2004). Indeed, as mentioned above, the experimental results show that strong axisymmetric forcing can also trigger similar turbulent structures such as puffs and slugs (Leite 1959, Fox *et al* 1968).

In light of the studies mentioned above, I propose to describe axisymmetric nonlinear near-neutral modes in pipe flows from a point of view that draws from recent work on exact wave solutions of nonlinear partial differential equations (PDEs) via the inverse scattering transform (IST). For some of them, integrability holds and the IST unveils the dynamics of solitons and travelling waves (see, e.g., Ablowitz *et al* 1974, Ablowitz and Segur 1981, Drazin and Johnson 1990). Among the integrable PDEs, the Korteweg–de Vries (KdV) equation

$$\partial_t u + \partial_{xxx} u + 6u\partial_x u = 0$$

arises as a fundamental mathematical model governing the propagation of waves in shallow waters, long waves in a density-stratified ocean, ion and acoustic waves in a plasma or acoustic waves on a crystal lattice. It admits the *cnoidal* periodic wave solution equation (see, e.g., Drazin and Johnson 1990)

$$u(x,t) = \frac{c}{2}\mathrm{cn}\,(\zeta, M)\,, \quad \zeta = \frac{\sqrt{c}}{2}\,(x - ct)\,, \tag{1}$$

where $\mathrm{cn}(\zeta, M)$ is one of the Jacobi elliptic functions of modulus $0 \leqslant M \leqslant 1$, and c is the wave celerity. For $M = 1$, (1) reduces to the cnoidal soliton

$$u = \frac{c}{2}\mathrm{sech}^2(\zeta). \tag{2}$$

More generally, the long-term regime of KdV solutions can be completely identified via the IST as an active nonlinear state of elastically interacting solitons propagating through a cnoidal wave background. If integrability does not hold, direct perturbation theory (see, e.g., Keener and McLaughlin 1977, Kodama and Ablowitz 1981, Herman 1990a, Mann 1997a,b) or adiabatic approximation theory (see, e.g., Herman 1990b, Gerdjikov *et al* 2001) provides a mathematical framework for studying analytical solutions of non-integrable equations as weak perturbations of integrable ones. Indeed, many non-integrable equations also possess simple localized solutions that may be called solitons, solitary waves or dissipative solitons in which, for example, nonlinearities are balanced with dispersion and dissipation (see, e.g., Knobloch 2008).

Thus, drawing from the IST theory I attempt to explore the hypothesis of a Navier–Stokes flow defined as a nonlinear sea state (Fedele 2008, Fedele and Tayfun 2009) of interacting coherent wave structures of soliton-bearing equations. Such sea states may, for example, explain the occurrence of steady ‘puffs’ observed in both numerical simulations and experiments of turbulent pipe flows (Willis and Kerswell 2008, 2009). Indeed, the puff dynamics appears to be similar to that of a soliton. This loses energy as it interacts with the background or other solitons, and it delocalizes in space by splitting into many other smaller solitons, leading to a solitonic sea state. In numerical experiments of pipe flows at $Re \approx 10^5$, Duguet (2008) and Duguet *et al* (2008) also discovered ‘edge’ states in the form of localized travelling waves that neither relaminarize nor become turbulent. These appear to be ‘semi-stable’ solitary waves or solitons. Thus, for a better understanding of the transition to turbulence in pipe flows, it would be useful to attempt to unveil the existence of solitons and travelling waves of Navier–Stokes pipe flows and their associated dynamical equations. Recent studies by Ryzhov (2010) do so for the Blasius flows, which at high Reynolds numbers are described by a Benjamin–Davis–Acrivos integro-differential equation. This supports soliton structures that explain the formation of spikes observed in boundary-layer transition (Kachanov *et al* 1993).

In this paper, I present a similar study for the special case of non-rotating axisymmetric pipe flows, which aims at reducing the Navier–Stokes equations to soliton-bearing equations. The paper is structured as follows. I first introduce the stream function formulation for describing axisymmetric pipe flows. Then, I show that the associated equations can be reduced at high Reynolds numbers to weakly nonlinear coupled generalized KdV equations, which support travelling wave solutions as solitons and periodic waves. Finally, the interpretation of the associated vortical structures is discussed.

2. Axisymmetric Poiseuille pipe flow

Consider the axisymmetric motion of an incompressible fluid in a pipe of circular cross section of radius R driven by an imposed uniform pressure gradient $\partial_z P$. Define a cylindrical coordinate system (z, r, θ) with the z-axis along the streamwise direction, and (u, v, w) as the radial, azimuthal and streamwise velocity components and p is the pressure perturbation to P. Further, rescale the time, radial and streamwise lengths as well as velocities with T, R and U_0, respectively. Here, $T = R/U_0$ is a convective time scale and U_0 is the maximum laminar flow velocity. Neglecting the azimuthal velocity component v, the axisymmetric velocity field (independent of θ) can be expressed in terms of the Stokes stream function $\Psi(r, z, t)$ as

$$u = -\frac{1}{r}\frac{\partial \Psi}{\partial z}, \quad w = \frac{1}{r}\frac{\partial \Psi}{\partial r}, \tag{3}$$

and the condition of incompressibility is satisfied. In order to investigate the nonlinear behaviour of a perturbation superimposed on the base flow $W_0(r) = 1 - r^2$, the stream function is divided into two terms as

$$\Psi = \Psi_0 + \psi, \tag{4}$$

where $\Psi_0 = r^2(1 - r^2/2)/2$ represents the stream function of the laminar flow W_0, and ψ that of the disturbance. The following nonlinear equation for $\psi(z, r, t)$ can be derived from the Navier–Stokes equations as (Itoh 1977)

$$\partial_t \mathsf{L}\psi + W_0 \partial_z \mathsf{L}\psi - \frac{1}{Re}\mathsf{L}^2\psi = \mathcal{N}(\psi), \tag{5}$$

where the nonlinear differential operator

$$\mathcal{N}(\psi) = -r^{-1}\partial_r\psi\,\partial_z\mathsf{L}\psi + r^{-1}\partial_z\psi\,\partial_r\mathsf{L}\psi - 2r^{-2}\partial_z\psi\,\mathsf{L}\psi, \tag{6}$$

the linear operator

$$\mathsf{L} = \mathcal{L} + \partial_{zz}, \quad \mathcal{L} = \partial_{rr} - r^{-1}\partial_r = r\partial_r\left(r^{-1}\partial_r\right) \tag{7}$$

and Re is the Reynolds number based on U_0 and R. The boundary conditions for (5) reflect the boundedness of the flow at the centreline of the pipe and the no-slip condition at the wall, that is, $\partial_r\psi = \partial_z\psi = 0$ at $r = 1$.

Expanding the operator L, (5) can be written as

$$\partial_t\mathcal{L}\psi + \underbrace{W_0\partial_z\mathcal{L}\psi}_{\text{Convection}} + \underbrace{\partial_{tzz}\psi + W_0\partial_{zzz}\psi}_{\text{Dispersion}} - \underbrace{\frac{1}{Re}\mathsf{L}^2\psi}_{\text{Viscosity}}$$
$$= \underbrace{-r^{-1}\partial_r\psi\,\partial_z\mathcal{L}\psi + r^{-1}\partial_z\psi\,\partial_r\mathcal{L}\psi - 2r^{-2}\partial_z\psi\,\mathcal{L}\psi}_{\text{KdV-type nonlinearities } \sim\psi\partial_z\psi} + \text{HOT}. \tag{8}$$

Here, if one ignores the r dependence, differentiated terms in z are identified to be similar to those of KdV equations, i.e. convection, dispersion and nonlinearities proportional to $\psi\partial_z\psi$. In addition, viscous effects play a role and HOT represents higher-order nonlinearities of the type $\psi\partial_{zzz}\psi$ and $\partial_z\psi\partial_{zz}\psi$. It must be pointed out that, traditionally, the KdV equation arises, for example, from the shallow water equations (see, e.g., Drazin and Johnson 1990) whenever one studies the weakly nonlinear evolution of wave packets. In particular, the relevance or not of the KdV equation thus follows from the dispersion relation $\omega = \omega(k)$ of Fourier waves $\exp(\mathrm{i}kx - \mathrm{i}\omega t)$ when the wave packet's carrier wave $\exp(\mathrm{i}k_0 x)$ corresponds to an extremum of group velocity. For the nonlinear equation (8) there is no need to study amplitudes and phases of Fourier waves in order to appreciate the hidden KdV scaling that arises if nonlinearities balance out dispersion. Indeed, one can clearly realize that (8) is already in a generalized KdV-type form, whereas the shallow water equations are not.

To solve (8), consider a function space $\mathcal{S}$ as the span of a complete set of J generalized harmonics $\chi_j(r)$, and expand ψ as

$$\psi(r,z,t) = \sum_{j=1}^{J} g_j(z,t)\chi_j(r). \tag{9}$$

One can then average along the radial direction r by projecting (8) onto $\mathcal{S}$ and obtain the nonlinear equations governing the dynamics of the amplitudes g_j. In a multiple scale perturbation setting, the structure of (8) suggests the following KdV scaling for g_j in order to balance dispersion and nonlinearities:

$$g_j(z,t) \to \epsilon b_j(\xi,\tau), \tag{10}$$

where b_j is a new amplitude defined on the stretched reference frame

$$\xi = \epsilon^{1/2}(z - Vt), \qquad \tau = \epsilon^{3/2} t, \tag{11}$$

with ϵ being a small parameter and V denotes a convective speed to be properly chosen. As a result of the scalings (10) and (11), the axisymmetric Navier–Stokes equation (5) reduces to a set of coupled generalized KdV equations as shown below.

3. Reduction to KdV-type equations

The basis χ_j in (9) will be chosen as the eigenfunctions of a linear boundary value problem (BVP) defined as follows. If in (8) nonlinearities are neglected and the flow is assumed uniform in the streamwise direction, then the associated stream function $\psi_0(r,t)$ satisfies the linear PDE

$$\partial_t \mathcal{L}\psi_0 = \frac{1}{Re}\mathcal{L}^2\psi_0, \tag{12}$$

with the boundedness of $r^{-1}\psi_0$ and $r^{-1}\partial_r\psi_0$ at the pipe centreline, and $\psi_0 = \partial_r\psi_0 = 0$ at $r = 1$. The general solution of (12) is

$$\psi_0(r,t) = q_0\Psi_0(r) + \sum_{j=1}^{\infty} q_j\phi_j(r)\mathrm{e}^{-\lambda_j^2 t/Re}, \tag{13}$$

where q_j are arbitrary constants, Ψ_0 is the laminar stream function corresponding to a zero-eigenvalue eigenfunction and the basis ϕ_j (Stokes eigenmodes) satisfy the BVP

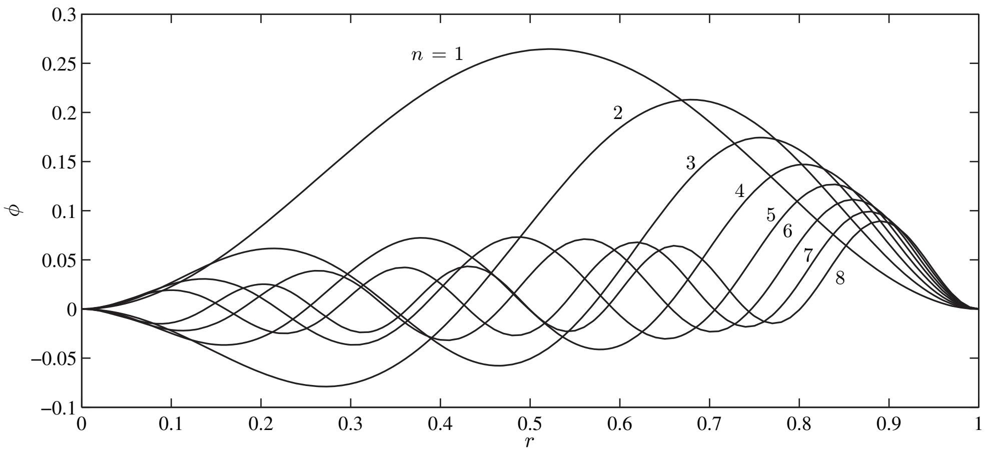

Figure 1. The five least stable Stokes eigenmodes of the eigenvalue problem (14).

(see appendix A)

$$\mathcal{L}^2\phi_j = -\lambda_j^2\mathcal{L}\phi_j, \tag{14}$$

with $r^{-1}\phi_j$ and $r^{-1}\partial_r\phi_j$ bounded at $r = 0^+$, and $\phi_j = \partial_r\phi_j = 0$ at $r = 1$. The positive eigenvalues λ_j are the roots of $J_2(\lambda_j) = 0$, where $J_2(r)$ is the Bessel function of the first kind of second order (see Abramowitz and Stegun 1972). For the first two least stable eigenmodes $\lambda_1 = 5.136$ and $\lambda_2 = 8.417$, respectively. The first five least stable eigenmodes, shown in figure 1, exhibit an increasing number of maxima that monotonically decrease towards the centre of the pipe. Further, higher and more damped 'wall modes' tend to localize toward $r = 1$. The function space $\mathcal{S}$, span of the set of the generalized harmonics ϕ_j, is a Hilbert space supported by the inner product

$$\langle\varphi_1, \varphi_2\rangle = -\int_0^1 \varphi_1\, \mathcal{L}\varphi_2\, r^{-1}\,\mathrm{d}r = \int_0^1 \partial_r\varphi_1\partial_r\varphi_2 r^{-1}\,\mathrm{d}r, \tag{15}$$

and the associated eigenfunctions form a complete and orthonormal set. Note that Ψ_0 makes the null space of the operator $\mathcal{L}^2$ and also denotes the steady-state solution of (12). According to (12), the cross-sectional area average $\overline{w}^r = 2\int_0^1 (r)\ w\,\mathrm{d}r$ of the streamwise velocity $w = \frac{1}{r}\frac{\mathrm{d}\phi_n}{r}$ associated with each eigenfunction ϕ_n vanishes, but that of the corresponding streamwise pressure gradient does not because viscous stresses are not uniformly distributed across the pipe section as the local streamwise acceleration forces. To conserve the mass flux of the laminar base state, q_0 must be set equal to zero. Then, the perturbation ψ_0 is given by the sum of viscous non-normal eigenmodes that exponentially decay in time and the laminar flow is linearly stable (see, e.g., Itoh 1977, Drazin and Reid 1981).

To solve for the nonlinear equation (8) the basis χ_j in (9) are chosen as the Stokes eigenmodes ϕ_j of (14). Since ϕ_j satisfies the pipe flow boundary conditions *a priori*, so does ψ of (9). The eigenmode amplitudes g_j in the expansion (9) depend upon both z and t and the number J of modes should be very large for the completeness of the eigenset. However, in the nonlinear regime, one can focus on the dynamics of the first few least stable modes as long as the perturbation amplitude g_j remains for all time in a small neighbourhood of zero (the laminar state). Indeed, in this case higher-order modes can be considered as slaved and will not affect the weakly nonlinear dynamics of the less stable modes. However, in general, higher damped modes cannot be neglected for finite-amplitude perturbations near a nontrivial fixed point, if any exists. Hereafter, only small flow perturbations of $O(\epsilon)$ near the laminar state are considered in order to legitimately neglect slaved modes.

The set of equations for g_j are obtained by Galerkin-projecting (5) onto $\mathcal{S}$ by means of the inner product (15). In accord with the scaling (10) and (11), the Galerkin equations in the new variables $b_j(z, \tau)$, correct to $O(\epsilon)$, reduce to the KdV-type system

$$\partial_\tau b_j + \tilde{\beta}_{jj}\partial_{\xi\xi\xi} b_j + \sum_{n,m} \tilde{F}_{jnm} b_n \partial_\xi b_m = \epsilon\left(-\frac{\mathcal{V}_j}{\epsilon^{5/2} Re} + \mathcal{N}_j\right), \tag{16}$$

where $\mathcal{N}_j$ accounts for higher-order terms of the type $b_n\partial_{\xi\xi\xi}b_m$ and $\partial_\xi b_n \partial_{\xi\xi} b_m$,

$$\mathcal{V}_j = \sum_m \tilde{\lambda}^2_{jm} b_m, \tag{17}$$

and indices in any sum implicitly run between 1 and J. The derivation of (16) and the coefficients $\tilde{F}_{jnm}$, $\tilde{\beta}_{jj}$ and $\tilde{\lambda}^2_{jm}$ are given in appendix C. As $Re \to \infty$, if $\epsilon \sim O(Re^{-2/5})$, then (16) reduces to

$$\partial_\tau b_j + \tilde{\beta}_{jj}\partial_{\xi\xi\xi} b_j + \sum_{n,m} \tilde{F}_{jnm} b_n \partial_\xi b_m = \epsilon\left(-\mathcal{V}_j + \mathcal{N}_j\right), \tag{18}$$

where the viscous part $\mathcal{V}_j$ is of the same order as the nonlinear $\mathcal{N}_j$. Note that (18) is in general non-Hamiltonian and non-integrable. However, for special cases it may represent coupled/uncoupled Camassa–Holm equations (Camassa and Holm 1993) or KdV equations (see, e.g., Drazin and Johnson 1990) that are both integrable.

4. Inviscid travelling waves

If one ignores both $O(\epsilon)$ viscous and nonlinear terms in (18), then the inviscid dynamics of the perturbation is governed by the KdV-type system

$$\partial_t b_j + \tilde{\beta}_{jj}\partial_{\xi\xi\xi} b_j + \sum_{n,m} \tilde{F}_{jnm} b_n \partial_\xi b_m = 0. \tag{19}$$

The complete integrability of this system may hold only for particular forms of the tensor $\tilde{F}_{jnm}$. In the general case, (19) may still possess localized travelling waves that may be called solitons or solitary waves. To proceed analytically, drawing from Lou *et al* (2006), travelling waves of (19) are sought as related to solutions of the nonlinear Klein–Gordon (NKG) equation in the form

$$b_j = k^2\left[p_j + x_j \Phi^2(\zeta)\right], \quad j = 1, \ldots, J. \tag{20}$$

Here, $\zeta = k(\xi - c\tau)$ and Φ satisfies the NKG equation (see, e.g., Lou and Ni 1989)

$$\left(\partial_\zeta \Phi\right)^2 = \mu\Phi^2 + \frac{\lambda}{2}\Phi^4 + \rho, \tag{21}$$

where the wave speed c, the coefficients k, p_j, x_j and the triplet $\{\mu, \lambda, \rho\}$ are free parameters to be determined. Substituting (20) into (19) yields

$$\mathcal{R}_j \Phi\, \partial_\zeta \Phi + \mathcal{S}_j \Phi^3\, \partial_\zeta \Phi = 0, \tag{22}$$

where

$$\mathcal{R}_j = -ck^3 x_j + 4\mu k^5 \tilde{\beta}_{jj} x_j + k^5 \sum_{n,m} \tilde{F}_{jnm} p_n x_m, \tag{23}$$

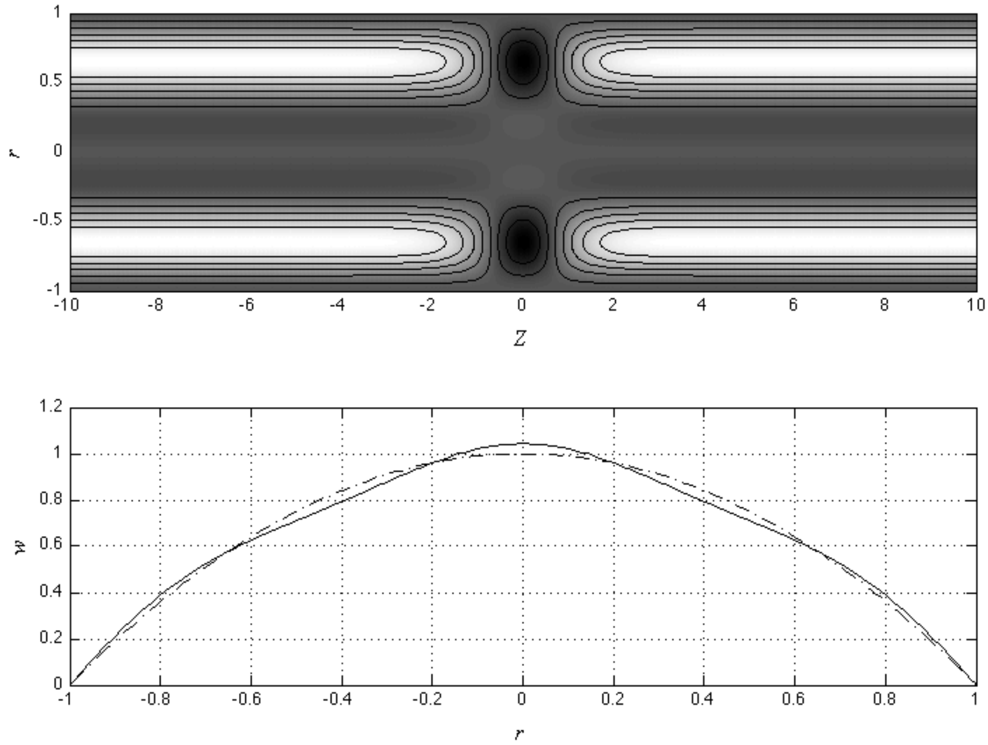

Figure 2. The cn-soliton of equation (29), wall mode: (top) contour plot of ψ_{d} and (bottom) velocity profiles of the perturbed (solid) and laminar (dash) flows.

$$\mathcal{S}_j = 6\lambda k^5 \tilde{\beta}_{jj} x_j + k^5 \sum_{n,m} \tilde{F}_{jnm} x_n x_m. \tag{24}$$

Note that (22) must be satisfied for any choice of the function Φ. Thus, both (23) and (24) must vanish. In particular, $\mathcal{S}_j = 0$ yields a set of equations for J hyperconics Γ_j in $\mathbb{R}^J$ given by

$$6\lambda \tilde{\beta}_{jj} x_j + \sum_{n,m} \tilde{F}_{jnm} x_n x_m = 0, \qquad j = 1, \ldots, J, \tag{25}$$

to be solved for the coefficients x_n (see appendix B for the case $J = 2$). Further, $\mathcal{R}_j = 0$ leads to a linear system

$$(-c + 4\eta k^2 \tilde{\beta}_{jj}) x_j + k^2 \sum_{n,m} \tilde{F}_{jnm} p_n x_m = 0, \qquad j = 1, \ldots, J, \tag{26}$$

which can be solved to determine p_n, given the celerity c. For steady solutions (in the reference frame of ξ), $c = 0$, and (26) is satisfied by

$$p_n = \frac{2\eta\, x_n}{3\lambda}.$$

As a result, the KdV system (19) admits an infinite family of travelling wave solutions by a proper choice of the triplet (μ, λ, ρ), which yields Φ as a solution of the NKG equation (21) in terms of the Jacobi elliptic functions $\mathrm{cn}(\zeta)$, $\mathrm{sn}(\zeta)$ and $\mathrm{dn}(\zeta)$ with

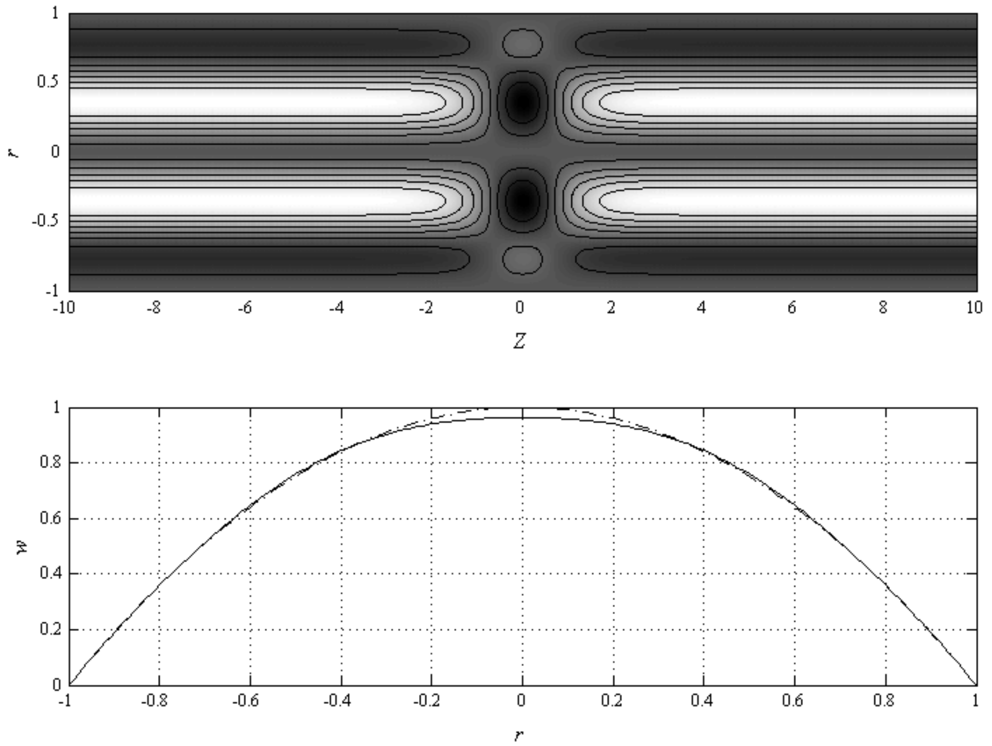

Figure 3. The cn-soliton of equation (29), centre mode: the same as in figure 2.

modulus $0 \leqslant M \leqslant 1$ (see Lou and Ni 1989). As an example, consider the two triplets $\{2M^2 - 1, -2M^2, 1 - M^2\}$ and $\{2 - M^2, -2, -1 + M^2\}$, which yield two sets of exact solutions given by, respectively,

$$b_j^{\mathrm{I}}(\xi, \tau) = k^2 x_j \left[-\frac{2M^2 - 1}{3M^2} + \mathrm{cn}^2(k\xi) \right] \tag{27}$$

and

$$b_j^{\mathrm{II}}(\xi, \tau) = k^2 x_j \left[-\frac{4M^2 - 2}{6} + \mathrm{dn}^2(k\xi) \right], \tag{28}$$

with k and M being free parameters. For $M = 1$, they both reduce to the family of sech-solitons

$$b_j^{\mathrm{III,s}}(\xi, \tau) = -\tfrac{1}{3} k^2 x_j + k^2 x_j \, \mathrm{sech}^2(k\xi). \tag{29}$$

The triplet $\{-(1 + M^2)/4, M/2, M/4\}$ provides a more complicated form of travelling wave, viz

$$b_j^{\mathrm{IV}}(\xi, \tau) = k^2 x_j \left[-\frac{4M^2 + 4}{12M} + \frac{4M^2[1 + M\,\mathrm{sn}(k\xi)]^2[1 + \mathrm{sn}(k\xi)]^2}{\left(\sqrt{1+M}[1 + M\,\mathrm{sn}(k\xi)] + \sqrt{1-M}\,\mathrm{dn}(k\xi)]\right)^2} \right]. \tag{30}$$

As M approaches 1, b_j^{IV} also tends to a soliton shape similar to (29).

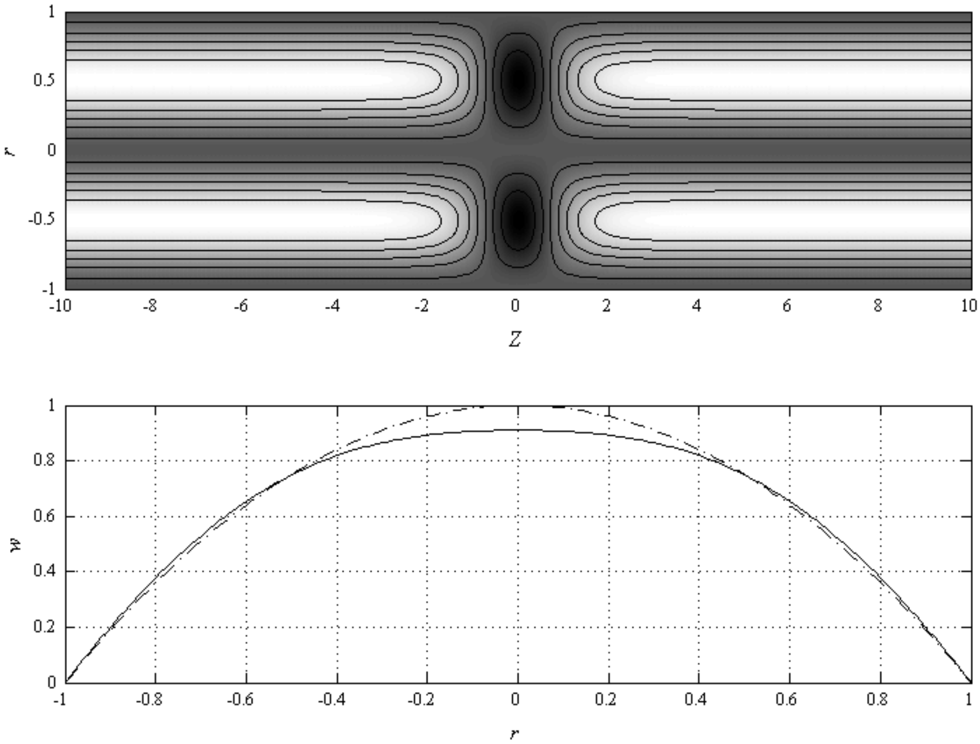

Figure 4. The cn-soliton of equation (29), mixed mode: the same as in figure 2.

5. $O(\epsilon)$-dynamics of solitary waves

Hereafter, it will be shown that the higher-order terms $\mathcal{N}_j$ in (18) do not have any role in the weakly nonlinear dynamics of the inviscid solitary waves (29). In the Galilean reference frame (ξ, τ), the disturbances just decay due to viscous dissipation on the time scale $\tau \sim O(\epsilon^{-1})$. Similar conclusions also hold for the limiting soliton form of (30). To proceed to a tractable analytical solution of (18) via perturbation methods, define the new variable

$$\tilde{b}_j = b_j + \tfrac{1}{3}k^2 x_j, \tag{31}$$

which satisfies

$$\partial_\tau \tilde{b}_j + \tilde{\beta}_{jj}\partial_{\xi\xi\xi}\tilde{b}_j + \sum_{n,m}(\tilde{L}_{jnm}\partial_\xi \tilde{b}_m + \tilde{F}_{jnm}\tilde{b}_n\partial_\xi \tilde{b}_m) = \epsilon\tilde{\mathcal{F}}_j, \tag{32}$$

with $\tilde{L}_{jnm} = k^2 x_n \tilde{F}_{jnm} x_n/3$ and

$$\tilde{\mathcal{F}}_j = \sum_m \tilde{\lambda}^2_{jm}(k^2 x_m/3 - \tilde{b}_m) + \mathcal{N}_j. \tag{33}$$

From (29), the $O(1)$ unperturbed equations (32) admit the soliton solutions

$$\tilde{b}_j = b_j + \tfrac{1}{3}k^2 x_j = k^2 x_j\,\mathrm{sech}^2(k\xi). \tag{34}$$

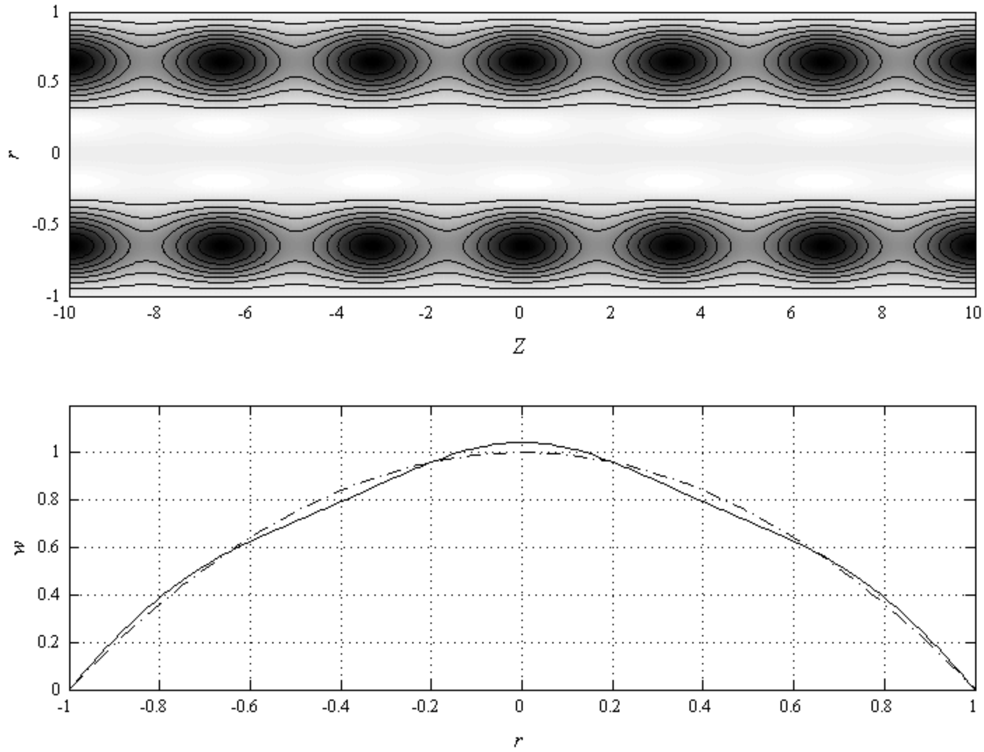

Figure 5. The dn-travelling wave of equation (28), wall mode ($M = 0.2$): the same as in figure 2.

To determine the effects of the perturbation terms in (32) on the dynamics of the unperturbed soliton $\tilde{b}_j$, assume that $k(\tau_2)$ varies on the slow viscous time scale $\tau_2 = \epsilon\tau = \epsilon^{5/2}t$. The evolution of k is derived by means of adiabatic approximation theory as follows (see, e.g., Herman 1990b, Gerdjikov *et al* 2001). The rate of change in the pseudo energy

$$E = \frac{1}{2}\sum_j \int_{-\infty}^{\infty} \tilde{b}_j^2 \, d\xi = \frac{2k^3}{3}\sum_n x_n^2 \tag{35}$$

is given by

$$\frac{dE}{d\tau_2} = \sum_j \int_{-\infty}^{\infty} \tilde{b}_j \partial_\tau \tilde{b}_j \, d\xi. \tag{36}$$

Using (32) and (34), this yields after some algebra and integration by parts the dynamical equation for k

$$\frac{dk}{d\tau_2} = \frac{\gamma}{3}k, \tag{37}$$

where

$$\gamma = -\frac{\sum_{n,m} \tilde{\lambda}_{nm}^2 x_n x_m}{\sum_n x_n^2}. \tag{38}$$

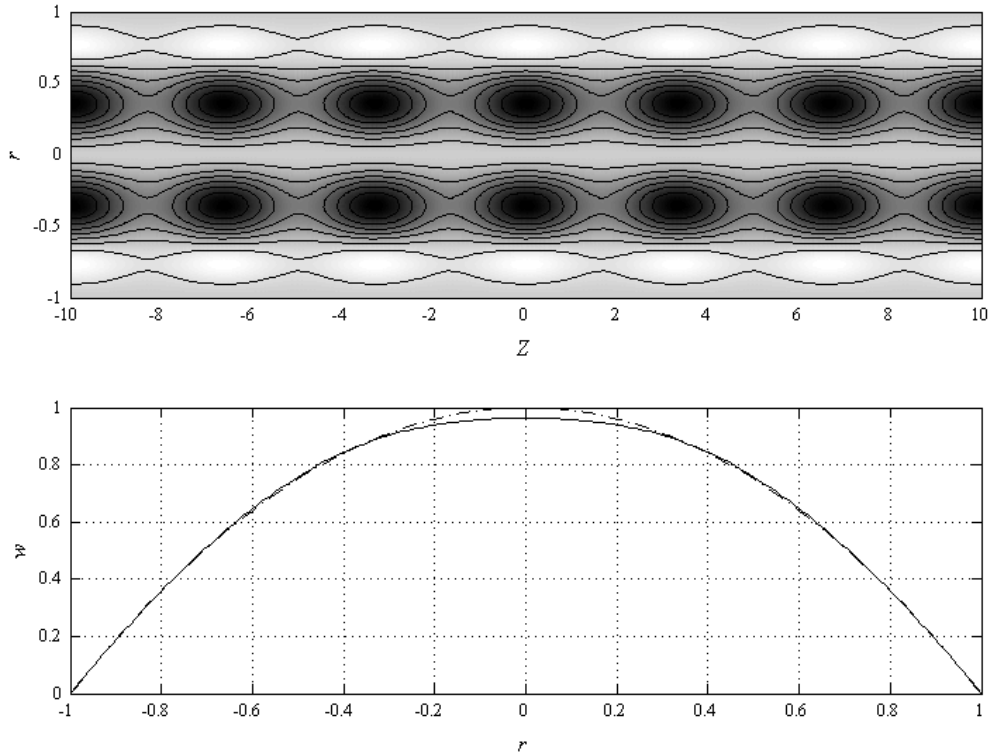

Figure 6. The dn-travelling wave of equation (28), centre mode ($M = 0.2$): the same as in figure 2.

Note that (37) can also be derived from direct perturbation theory (Keener and McLaughlin 1977, Kodama and Ablowitz 1981, Herman 1990a, Mann 1997a,b). The solution of (37) follows as

$$k(t) = k_0 \exp\left(\frac{\gamma}{3}\epsilon^{5/2}t\right), \tag{39}$$

where k_0 is the soliton parameter. Numerical computations reveal that γ is negative so that as $Re \to \infty$, an inviscid soliton of small amplitude $\epsilon \sim O(Re^{-2/5})$ is affected by viscous dissipation only on the very long time scale $t \sim O(\epsilon^{-2.5}) = O(Re^{6.25})$. As a result, the soliton structures can be assumed to behave inviscidly on shorter time scales, but they will eventually decay. Similar conclusions also hold for their periodic counterparts.

6. Nonlinear modes

The stream function ψ_d of the generic cnoidal wave disturbance follows from (9) and (20) as

$$\psi_d(r, Z) = \psi/(\epsilon k^2) = \left[\frac{2\mu}{3\lambda} + \Phi^2(Z)\right]\sum_{j=1}^{J} x_j\phi_j, \tag{40}$$

where, owing to the KdV scaling (11), $Z = \epsilon^{1/2}(z - Vt)$ denotes a reference frame moving with the perturbation at the speed V and J denotes the number of eigenmodes. Since the Stokes eigenmodes ϕ_j are strongly damped (see, for example, Fedele *et al* 2005), consider

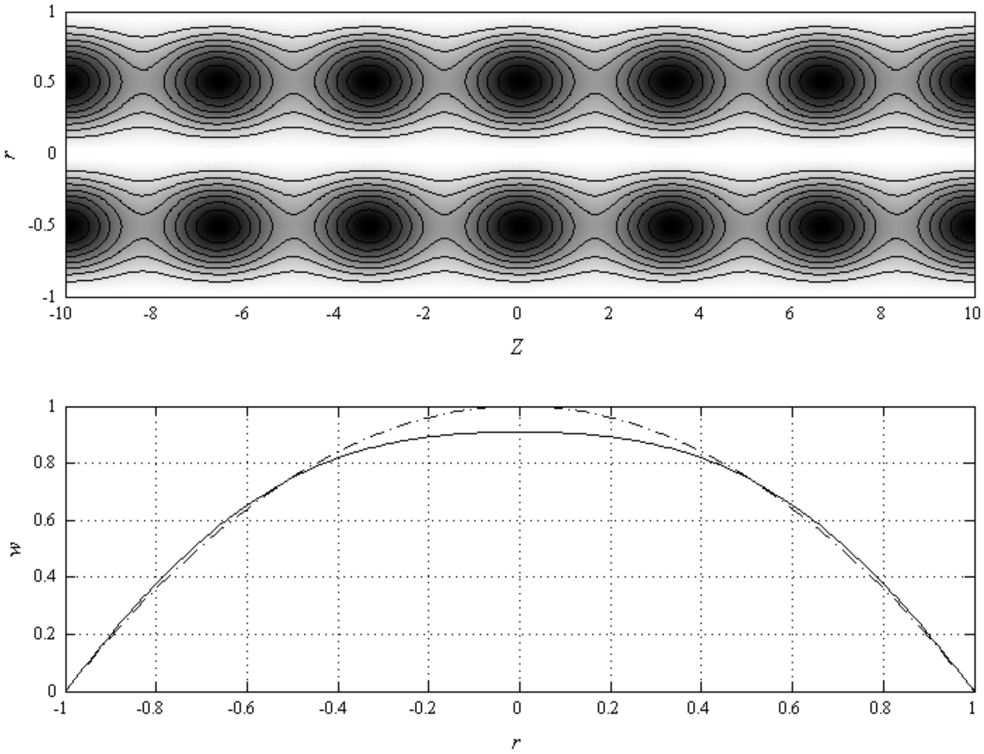

Figure 7. The dn-travelling wave of equation (28), mixed mode ($M = 0.2$): the same as in figure 2.

the weakly nonlinear dynamics of the amplitudes in (19) for the first $J = 2$ least stable modes ϕ_1 ($\lambda_1 = 5.136$) and ϕ_2 ($\lambda_2 = 8.417$), respectively. Solving (25) yields three nontrivial travelling wave solutions with the factor γ negative and equal to -8.49, -20.96 and -23.89, respectively (see appendix D). In physical space, $\psi_{\rm d}$ represents a localized/periodic toroidal vortex tube travelling with the celerity $V \simeq 0.77U_0$, U_0 being the maximum laminar flow speed. In particular, the disturbance travels faster than the average laminar flow speed $\sim U_0/2$. Further, the streamwise velocity $w_{\rm d}$ of the disturbance is given by

$$w_{\rm d}(r, Z) = \frac{1}{r}\frac{\partial \psi_d}{\partial r} = \left[\frac{2\mu}{3\lambda} + \Phi^2(Z)\right]\frac{1}{r}\sum_{j=1}^{J} x_j \frac{{\rm d}\phi_j}{{\rm d}r}. \tag{41}$$

The radial average $\overline{w_d}^r$ is null and the mass flux is conserved through the pipe, where $\overline{w_{\rm d}}^r = 2\int_0^1 r\, w_d(r, Z){\rm d}r$. However, the streamwise mean $\overline{w_{\rm d}}^Z$ is non-zero

$$\overline{w_d}^Z(r) = \lim_{L\to\infty}\frac{\int_{-L/2}^{L/2} w_d(r, Z){\rm d}Z}{L} = \frac{2\mu}{3\lambda r}\sum_{j=1}^{J} x_j \frac{{\rm d}\phi_j}{{\rm d}r}, \tag{42}$$

and so is the cross-sectional area-average of the streamwise perturbation pressure gradient. The contours of $\psi_{\rm d}$ for each of the three vortical structures associated with the sech-soliton (29) are shown in figures 2–4, respectively. In the same figures, the streamwise velocity profiles at $Z = 0$ of both the perturbed and laminar flows are also shown. From (28), their dn-periodic counterparts are shown in figures 5–8; the cn-periodic solutions of (27) yield

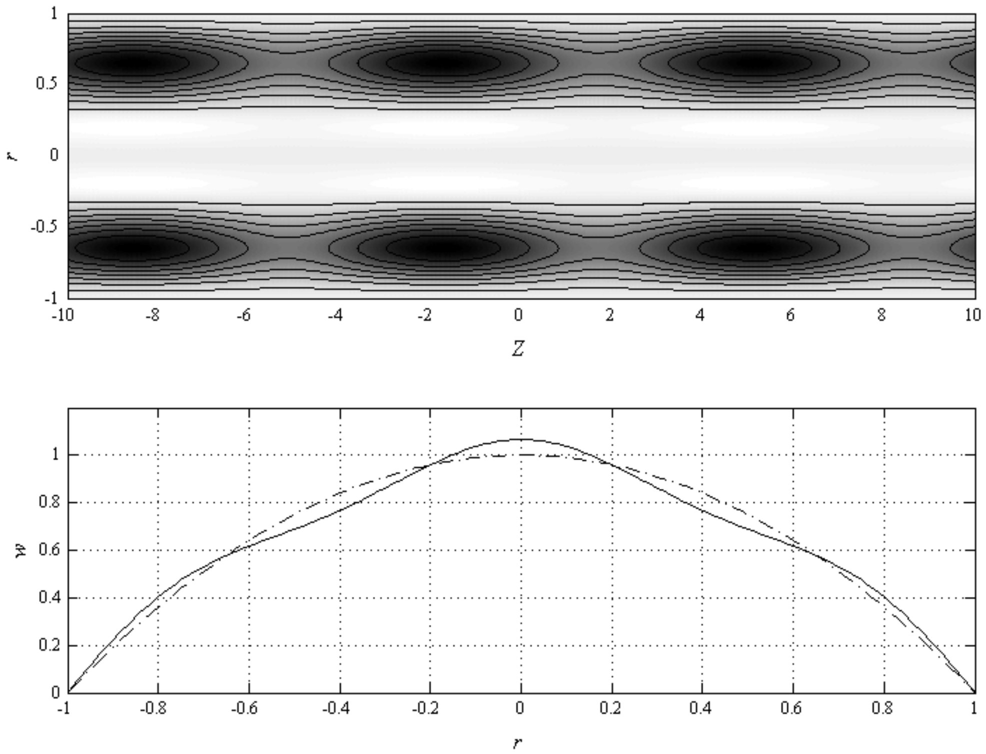

Figure 8. Travelling wave of equation (30), wall mode ($M = 0.3$): the same as in figure 2.

structures with the same topology and are not shown here. In particular, figure 2 shows a vortical structure localized near the wall (wall mode, $\gamma = -23.89$), whereas that of figure 3 wraps around the pipe axis (centre mode, $\gamma = -20.96$). The soliton structure of figure 4 fills the cross-section almost entirely as a superposition of a wall and a centre mode (mixed mode) and it is also the least stable mode in the viscous regime ($\gamma = -8.49$). A similar classification also holds for their dn-periodic counterparts (28) as clearly seen from figures 5–8, as well as for the travelling waves of (30) shown in figures 8–10. Clearly, the perturbed flow (laminar+vortex) shows a signature of axisymmetric streaks, especially the wall modes.

7. Conclusions

It is shown that the axisymmetric Navier–Stokes equations can be related to soliton-bearing equations. A generic perturbation to the laminar state is expanded in the Fourier sum of (linearly stable) Stokes modes with amplitudes varying in both the streamwise direction and time. As $Re \to \infty$, the nonlinear dynamics of a small perturbation of $\epsilon \sim O(Re^{-2/5})$ can be reduced to that of the first few least stable modes neglecting the interactions with higher damped modes, which can be set as slaved. For time scales much less than $t \sim O(\epsilon^{-2.5}) = O(Re^{6.25})$, the dynamics is primarily inviscid and governed by a set of KdV-type equations. These support nonlinear travelling waves, which in physical space represent localized/periodic toroidal vortices that travel slightly slower than the maximum laminar flow speed. The vortical structures are localized near the wall (wall mode) or wrap around the pipe

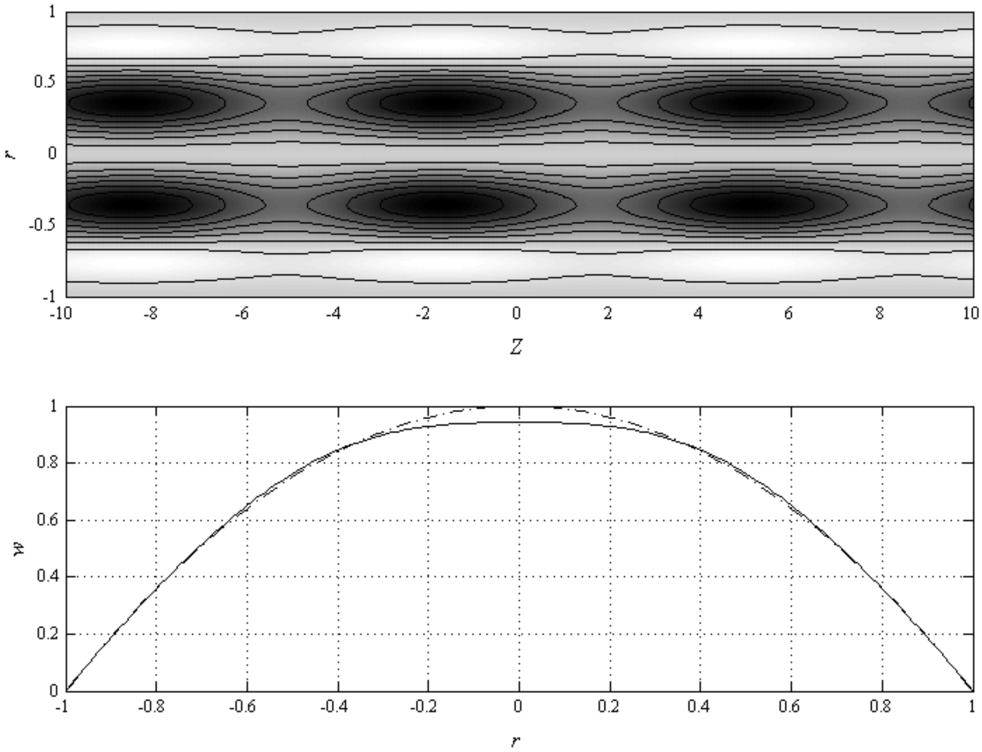

Figure 9. Travelling wave of equation (30), centre mode ($M = 0.3$): the same as in figure 2.

axis (centre mode). They have a non-zero streamwise mean, but they radially average to zero to conserve mass flux through the pipe.

On the one hand, the wall modes may be interpreted as the axisymmetric analogue of the two-dimensional (2D) rolls+streaks stage of the self-sustaining process (SSP) of Waleffe (1995a,b) in Couette flows or that of Wedin and Kerswell (2004) in pipe flows. However, in SSPs the streaks generated by streamwise rolls are unstable to spanwise perturbations, which trigger the nonlinear regeneration of rolls so that the process can sustain itself. On the other hand, the periodic centre modes as those of figures 6 and 9 may be related to the neutral centre modes discovered by Walton (2011) in unsteady pipe flows, inviscid axisymmetric slug structures similar to those proposed by Smith *et al* (1990). Walton's slug modes emerge from the wall layer as the disturbance amplitude is increased, eventually tending to concentrate along the pipe centreline and propagating downstream at almost the maximum laminar fluid velocity. As suggested by Walton (2011), the slug modes most likely represent unstable equilibrium states.

If the inviscid nonlinear modes found in this work are proven to be unstable to non-axisymmetric perturbations, that would also suggest the existence of a new SSP, where poloidal disturbances nonlinearly sustain toroidal vortices. To investigate this possibility, it would be useful to start with the investigation of a simpler three-component but still 2D flow disturbance with no azimuthal dependence. In this case, the velocity field

$$\mathbf{u}(r, z, t) = \left(-\frac{1}{r}\partial_z\psi, v, \frac{1}{r}\partial_r\psi\right) \tag{43}$$

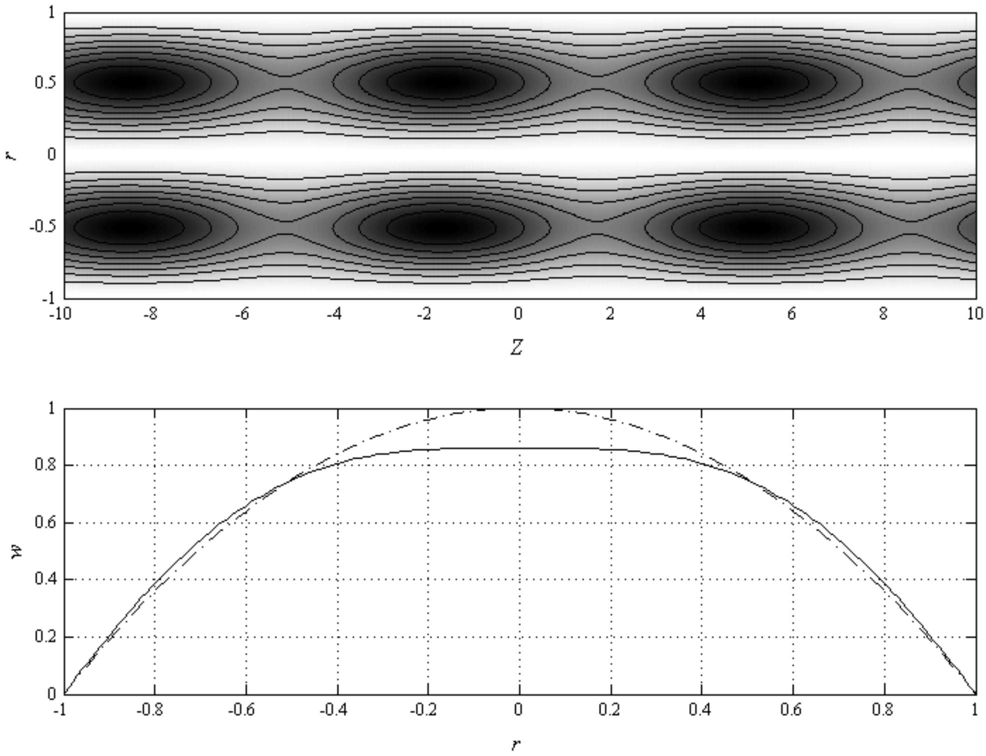

Figure 10. Travelling wave of equation (30), mixed mode ($M = 0.3$): the same as in figure 2.

can be written in terms of the stream function ψ for the axisymmetric part of the flow as in (3) and the azimuthal velocity component v. From the Navier–Stokes equations, ψ and v satisfy

$$\partial_t \mathsf{L}\psi + W_0 \partial_z \mathsf{L}\psi - \frac{1}{Re}\mathsf{L}^2\psi = \mathcal{N}(\psi) - r^{-1}\partial_z v^2,$$
$$\partial_t v + W_0 \partial_z v - \frac{1}{Re}\mathsf{L}_1 v + r^{-1}\partial_r\psi\partial_z v + r^{-1}\partial_z\psi(\partial_r v + r^{-1}v) = 0, \tag{44}$$

where $\mathsf{L}_1 = r^{-1}\partial_r(r\partial_r) + \partial_{zz} - r^{-2}$. Without toroidal disturbances any poloidal perturbation v acts as a passive scalar and dissipates on the time scale $t \sim O(Re^{-1})$. As shown in this work, an inviscid toroidal vortical structure of $\epsilon \sim O(Re^{-2/5})$ dissipates on a much longer time scale $t \sim O(\epsilon^{-2.5}) = O(Re^{6.25})$. Thus, it may counterbalance the dissipation of v, which in turn can destabilize the vortex before viscous effects become appreciable. Work is in progress to carry out a Galerkin reduction of the system (44). Preliminary results (to be confirmed elsewhere) indicate that the poloidal component is indeed unstable to the toroidal travelling waves (40), suggesting that the system (44) may support a new SSP, as a possible precursor of puffs and slugs seen experimentally.

Finally, it is worth noting that the KdV system (18) can be extended to the case of developing laminar pipe flows treated by Walton (2011), with the coefficients $\tilde{\beta}_{jj}(\tau_2)$ and the speed $V(\tau_2)$ slowly varying on the viscous time scale $\tau_2 = \epsilon\tau$ and growing from zero to the values for fully developed Poiseuille flow. These are the two coefficients of the KdV system that are functions of the base flow. The leading order travelling wave solution is still given by (20), but now both k and x_j depend upon the slow time scale τ_2, since x_j is a function of $\tilde{\beta}_{jj}$ via the constraint (25). The evolution equations for x_j follow by differentiating (25) with respect to τ_2 and are coupled to the adiabatic equation for k given in (37), which itself contains an extra term that arises from the differentiation of x_j in the energy (35). Such an analysis is beyond the scope of this work and will be discussed elsewhere, but it suggests that the asymptotic technique presented here may be applicable to other stability problems.

Acknowledgments

The comments of the anonymous referee are acknowledged gratefully.

Appendix A

Consider the factorization of (14) as

$$\mathcal{L}\left(\mathcal{L}+\lambda^2\right)\phi = 0. \tag{A.1}$$

The general solution is given by $\phi = f_1 + f_2$ such that $\mathcal{L} f_1 = 0$ and $\left(\mathcal{L}+\lambda^2\right) f_2 = 0$, i.e.

$$\phi = C_1 + C_2 r^2 + C_3 r\, Y_1(\lambda r) + C_4 r\, J_1(\lambda r), \tag{A.2}$$

where, respectively, $Y_1(r)$ and $J_1(r)$ are the Bessel functions of the first kind (see Abramowitz and Stegun 1972) and C_1, C_2,C_3 and C_4 are constants to be determined by the boundary conditions. Since both the functions, $\frac{\phi}{r}$ and $\frac{1}{r}\frac{\mathrm{d}\phi}{\mathrm{d}r}$, must tend to zero as $r \to 0^+$, then $C_1 = C_3 = 0$. On the other hand, from the boundary conditions at $r = 1$, namely $\frac{\phi}{r} = \frac{1}{r}\frac{\mathrm{d}\phi}{\mathrm{d}r} = 0$, the following homogeneous linear system for the unknowns (C_2, C_4) emerges:

$$\begin{cases} C_2 + J_1(\lambda)\, C_4 = 0, \\ 2C_2 + [J_1(\lambda) + \chi J_0(\lambda) - J_1(\lambda)]\, C_4 = 0. \end{cases} \tag{A.3}$$

Non-trivial solutions exist if and only if $J_2(\lambda) = 0$ with $J_2(r)$ being the Bessel function of the first kind (see Abramowitz and Stegun 1972). Consequently, there are infinitely many roots or eigenvalues λ_n, $n = 1, 2, 3, \ldots$. The corresponding eigenfunctions can be expressed as

$$\phi_n = c_n \left[r^2 - \frac{r J_1(\lambda_n r)}{J_1(\lambda_n)} \right], \tag{A.4}$$

where c_n are constants. The set $\{\phi_n\}$ is orthonormal with respect to the scalar product (15) provided one chooses $c_n = \frac{\sqrt{2}}{\lambda_n}$.

Appendix B

To obtain the Galerkin equations for g_j, equation (5) is projected onto $\mathcal{S}$ by means of the inner product (15). This yields the vector system

$$\partial_t \mathbf{g} + \mathbf{C}\partial_z \mathbf{g} - \mathbf{A}\partial_{zzt}\mathbf{g} + \mathbf{B}\partial_{zzz}\mathbf{g} + \frac{1}{Re}\left(\mathbf{\Lambda g} - 2\partial_{zz}\mathbf{g} + \mathbf{A}\partial_{zzzz}\mathbf{g}\right) + \mathbf{f}_{1,z}(\mathbf{g}) + \mathbf{f}_{2,z}(\mathbf{g}) = \mathbf{0}, \tag{B.1}$$

where the $(J \times 1)$ column vectors $\mathbf{g}$, $\mathbf{f}_1$ and $\mathbf{f}_2$ are given by, respectively,

$$\left[\mathbf{g}\right]_j = g_j, \quad \left[\mathbf{f}_{1,z}\right]_j = \mathbf{g}^{\mathrm{T}}\mathbf{F}_j \partial_z \mathbf{g}, \quad \left[\mathbf{f}_{2,z}\right]_j = \partial_z \mathbf{g}^T \mathbf{G}_j \partial_{zz}\mathbf{g} + \mathbf{g}^{\mathrm{T}}\mathbf{H}_j \partial_{zzz}\mathbf{g}, \tag{B.2}$$

and the $(J \times J)$ matrices $\mathbf{A}$, $\mathbf{B}$, $\mathbf{C}$, $\mathbf{\Lambda}$, $\mathbf{F}_j$, $\mathbf{G}_j$ and $\mathbf{H}_j$ are given in appendix C. It is convenient to diagonalize the convective term $\partial_z \mathbf{g}$ in (B.1) via the variable transformation

$$\mathbf{g} = \mathbf{Q}\mathbf{a}, \tag{B.3}$$

where $\mathbf{Q}$ is the eigenvector matrix of $\mathbf{C}$ with elements q_{ij}, i.e. $\mathbf{C} = \mathbf{Q}\mathbf{V}\mathbf{Q}^{-1}$, and $\mathbf{V}$ is the eigenvalue matrix with diagonal elements $\hat{c}_j$. This leads to

$$\partial_t \mathbf{a} + \mathbf{V}\partial_z \mathbf{a} - \hat{\mathbf{A}}\partial_{zzt}\mathbf{a} + \hat{\mathbf{B}}\partial_{zzz}\mathbf{a} + \frac{1}{Re}(\hat{\mathbf{\Lambda}}\mathbf{a} - 2\partial_{zz}\mathbf{a} + \hat{\mathbf{A}}\partial_{zzzz}\mathbf{a}) + \mathbf{Q}^{-1}\mathbf{f}_{1,z}(\mathbf{Q}\mathbf{a}) + \mathbf{Q}^{-1}\mathbf{f}_{2,z}(\mathbf{Q}\mathbf{a}) = \mathbf{0}, \tag{B.4}$$

where $\hat{\mathbf{X}} = \mathbf{Q}^{-1}\mathbf{X}\mathbf{Q}$ for $\mathbf{X} = \mathbf{A}$, $\mathbf{B}$ and $\mathbf{\Lambda}$. The convective velocities $\hat{c}_j$ of each eigenmode in $\mathbf{V}$ are very close to their average speed

$$V = \frac{\sum_j \hat{c}_j}{J}, \tag{B.5}$$

Q3 with very good approximation up to $J = 4$, and the excess $\delta\mathbf{V} = (V\mathbf{I} - \mathbf{V})$ from V can be neglected since of $O(0.1)$ or less. Consider the rescaling (10)–(11) for a_j as

$$a_j(z, t) \to \epsilon a_j(\xi, \tau), \tag{B.6}$$

where the new space–time variables are given by

$$\xi = \epsilon^{1/2}(z - Vt), \qquad \tau = \epsilon^{3/2} t, \tag{B.7}$$

with V being the average speed defined in (B.5). As a result of (B.6), (B.7) and (B.5), (B.4) can be written as

$$\partial_\tau \mathbf{a} + \hat{\mathbf{B}}\partial_{\xi\xi\xi}\mathbf{a} + \mathbf{Q}^{-1}\mathbf{f}_{1,\xi}(\mathbf{Q}\mathbf{a}) = -\frac{1}{\epsilon^{3/2} Re}\hat{\mathbf{\Lambda}}\mathbf{a} + \epsilon\left(\delta\mathbf{V}\partial_\xi \mathbf{a} + \hat{\mathbf{A}}\partial_{\xi\xi\tau}\mathbf{a} - \mathbf{Q}^{-1}\mathbf{f}_{2,\xi}(\mathbf{Q}\mathbf{a})\right) + O(\epsilon^2). \tag{B.8}$$

Here, the excess $\delta\mathbf{V}$ from the average speed V appears at $O(\epsilon)$. It is convenient to further diagonalize the dispersive term $\partial_{\xi\xi\xi}\mathbf{a}$ by the variable transformation

$$\mathbf{a} = \mathbf{R}\mathbf{b}, \tag{B.9}$$

where $\mathbf{R}$ is the eigenvector matrix of $\hat{\mathbf{B}}$ with elements r_{ij}, i.e. $\hat{\mathbf{B}} = \mathbf{R}\mathbf{S}\mathbf{R}^{-1}$, and $\mathbf{S}$ is the eigenvalue matrix with elements $\tilde{\beta}_{jj}$. This leads to

$$\partial_\tau \mathbf{b} + \mathbf{S}\partial_{\xi\xi\xi}\mathbf{b} + \mathbf{T}^{-1}\mathbf{f}_{1,\xi}(\mathbf{T}\mathbf{b}) = -\frac{1}{\epsilon^{3/2} Re}\tilde{\mathbf{\Lambda}}\mathbf{b} + \delta\tilde{\mathbf{V}}\partial_\xi \mathbf{a} + \epsilon\left(\tilde{\mathbf{A}}\partial_{\xi\xi\tau}\mathbf{b} - \mathbf{T}^{-1}\mathbf{f}_{2,\xi}(\mathbf{T}\mathbf{b})\right) + O(\epsilon^2), \tag{B.10}$$

where $\mathbf{T} = \mathbf{Q}\mathbf{R}$, $\tilde{\mathbf{X}} = \mathbf{T}^{-1}\mathbf{X}\mathbf{T}$ for $\mathbf{X} = \mathbf{A}$ and $\mathbf{\Lambda}$, and $\delta\tilde{\mathbf{V}} = \mathbf{R}^{-1}\delta\mathbf{V}\mathbf{R}$. The matrix elements of $\mathbf{T}$, $\mathbf{T}^{-1}$, $\delta\tilde{\mathbf{V}}$, $\tilde{\mathbf{A}}$ and $\tilde{\mathbf{\Lambda}}$ are denoted by T_{jk}, $\tilde{T}_{jk}$, Δc_{jm}, $\tilde{\alpha}_{jm}$ and $\tilde{\lambda}^2_{jm}$, respectively. Further, from (B.3) and (B.9),

$$\mathbf{g} = \mathbf{T}\mathbf{b},$$

or equivalently

$$g_j = \sum_k T_{jk} b_k, \qquad j = 1, \ldots, J.$$

From (B.10), the scalar functions $b_j(z,\tau)$ satisfy the system

$$\partial_\tau b_j + \tilde{\beta}_{jj}\partial_{\xi\xi\xi} b_j + \sum_{n,m} \tilde{F}_{jnm} b_n \partial_\xi b_m = \epsilon\left(-\frac{\sum_{n,m}\tilde{\lambda}^2_{jm} b_m}{\epsilon^{5/2} Re} + \mathcal{N}_j\right), \tag{B.11}$$

with

$$\mathcal{N}_j = \sum_m (\Delta c_{jm}\partial_\xi b_m + \tilde{\alpha}_{jm}\partial_{\xi\xi\tau} b_m) - \sum_{n,m}(\tilde{G}_{jnm}\partial_\xi b_n \partial_{\xi\xi} b_m + \tilde{H}_{jnm} b_n \partial_{\xi\xi\xi} b_m),$$

where indices in any sum implicitly run between 1 and J,

$$\tilde{F}_{jnm} = \sum_{k,s,h} \tilde{T}_{jk} T_{sn} F_{ksh} T_{hm},$$

and similarly for $\tilde{G}_{jnm}$ and $\tilde{H}_{jnm}$.

Appendix C

$$[\mathbf{\Lambda}]_{jm} = \lambda_j^2 \delta_{im}, \quad [\mathbf{C}]_{jm} = c_{jm}, \quad [\mathbf{A}]_{jm} = \alpha_{jm}, \quad [\mathbf{B}]_{jm} = \beta_{jm},$$

$$\left[\mathbf{F}^{(j)}\right]_{nm} = F_{jnm}, \quad \left[\mathbf{G}^{(j)}\right]_{nm} = G_{jnm}, \quad \left[\mathbf{H}^{(j)}\right]_{nm} = H_{jnm},$$

where

$$c_{jm} = -\int_0^1 W_0 \phi_j \mathcal{L}\phi_m \, r^{-1}\,\mathrm{d}r, \quad \alpha_{jm} = \int_0^1 \phi_j\phi_m \, r^{-1}\,\mathrm{d}r, \quad \beta_{jm} = -\int_0^1 W_0\phi_j\phi_m \, r^{-1}\,\mathrm{d}r,$$

$$F_{jnm} = -\int_0^1 \phi_j \left[\partial_r\phi_n \mathcal{L}\phi_m - \partial_r(\mathcal{L}\phi_n)\phi_m + 2r^{-1}\mathcal{L}\phi_n\phi_m\right] r^{-2}\,\mathrm{d}r,$$

$$G_{jnm} = -\int_0^1 \phi_j\phi_m\partial_r\phi_n r^{-2}\,\mathrm{d}r, \quad H_{jnm} = -\int_0^1 \phi_j\left[-\phi_m\partial_r\phi_n + 2r^{-1}\phi_n\phi_m\right] r^{-2}\,\mathrm{d}r.$$

Appendix D

Consider now the case when $J = 2$. The algebraic system (25) reduces to a set of equations of two conics Γ_1 and Γ_2 in the Cartesian plane $(x_1 = X, x_2 = Y)$, that is,

$$\begin{cases} a_1 X^2 + b_1 Y^2 + c_1 XY + d_1 X = 0, & (\Gamma_1) \\ a_2 X^2 + b_2 Y^2 + c_2 XY + d_2 Y = 0, & (\Gamma_2) \end{cases} \tag{D.1}$$

where

$$a_1 = F_{111}, \quad b_1 = F_{122}, \quad c_1 = F_{112} + F_{121}, \quad d_1 = 6\lambda\tilde{\beta}_{11},$$
$$a_2 = F_{211}, \quad b_2 = F_{222}, \quad c_2 = F_{212} + F_{221}, \quad d_2 = 6\lambda\tilde{\beta}_{22}.$$

The two conics can be classified based on the sign of $C_j = a_j b_j - c_j^2/4$. In particular, for $j = 1, 2$ if $C_j > 0$ or $C_j < 0$, then Γ_j is an ellipse or a hyperbola, respectively. The case $C_j = 0$ is degenerate since the conic reduces to the locus of two intersecting lines. The solution for (X, Y) is given by the intersection $\Gamma_1 \cap \Gamma_2$. Further,

$$X = R\cos\theta, \quad Y = R\sin\theta,$$

where $t = \tan\theta$ satisfies the complete cubic equation

$$d_2 b_1 t^3 + (d_2 c_1 - d_1 b_2)t^2 + (d_2 a_1 - d_1 c_2)t - d_1 a_2 = 0 \qquad \text{(D.2)}$$

and

$$R = -\frac{d_1 \cos\theta}{a_1 \cos^2\theta + b_1 \sin^2\theta + c_1 \sin\theta\cos\theta}.$$

For Poiseuille flows, (D.2) admits three non-trivial simple real roots.

Q4 **References**

Ablowitz M J, Kaup D J, Newell A C and Segur H 1974 The inverse scattering transform-Fourier analysis for nonlinear problems *Stud. Appl. Math.* **53** 249

Ablowitz M J and Segur H 1981 *Solitons and the Inverse Scattering Transform (Studies in Applied Mathematics,* vol 4*)* (Philadelphia: SIAM)

Abramowitz M and Stegun I A 1972 *Handbook of Mathematical Functions* (New York: Dover) p 1046

Camassa R and Holm D D 1993 An integrable shallow water equation with peaked solitons *Phys. Rev. Lett.* **71** 1661

Cvitanović P 1995 Dynamical averaging in terms of periodic orbits *Physica* D **83** 109

Cvitanović P and Eckhardt B 1991 Periodic orbit expansions for classical smooth flows *J. Phys. A: Math. Gen.* **24** L237

Davey A 1978 On Itoh's finite amplitude stability theory for pipe flow *J. Fluid Mech.* **86** 695–703

Davey A and Nguyen H P F 1971 Finite-amplitude stability of pipe flow *J. Fluid Mech.* **45** 701

Duguet Y 2008 Lower-branch travelling waves and transition to turbulence in pipe flow *Isaac Newton Institute Workshop Wall Bounded Shear Flows: Transition and Turbulence* (HRT W01) Online at http://upload.sms.csx.cam.ac.uk/collection/132

Duguet Y, Willis A P and Kerswell R R 2008 Transition in pipe flow: the saddle structure on the boundary of turbulence *J. Fluid Mech.* **613** 255

Drazin P G and Johnson R S 1990 *Solitons: An Introduction* (Cambridge: Cambridge University Press)

Drazin P G and Reid W H 1981 *Hydrodynamic Stability* (Cambridge: Cambridge University Press)

Faisst H and Eckhardt B 2003 Travelling waves in pipe flow *Phys. Rev. Lett.* **91** 224502

Fedele F, Hitt D L and Prabhu R D 2005 Revisiting the stability of pulsatile pipe flow *Eur. J. Mech.* B **24** 237

Fedele F 2008 Rogue waves in oceanic turbulence *Physica* D **237** 2127

Fedele F and Tayfun M A 2009 Nonlinear wave groups and crest statistics *J. Fluid Mech.* **620** 221

Fox J A, Lessen M and Bhat W V 1968 Experimental investigation of the stability of Hagen–Poiseuille flow *Phys. Fluids* **11** 1–4

Gerdjikov V S, Doktorov E V and Yang J 2001 Adiabatic interaction of N ultrashort solitons: universality of the complex Toda chain model *Phys. Rev.* E **64** 056617–15

Gibson J F, Halcrow J and Cvitanovic P 2008 Visualizing the geometry of state space in plane Couette flow *J. Fluid Mech.* **611** 107

Kachanov Y S, Ryzhov O S and Smith F T 1993 Formation of solitons in transitional boundary layers: theory and experiment *J. Fluid Mech.* **251** 273

Keener J P and McLaughlin D W 1977 Solitons under perturbations *Phys. Rev.* A **16** 777

Kerswell R R 2005 Recent progress in understanding the transition to turbulence in a pipe *Nonlinearity* **18** R17

Kerswell R R and Tutty O R 2007 Recurrence of travelling waves in transitional pipe flow *J. Fluid Mech.* **584** 69

Knobloch E 2008 Spatially localized structures in dissipative systems: open problems *Nonlinearity* **21** T45–60

Kodama Y and Ablowitz M J 1981 Perturbations of solitons and solitary waves *Stud. Appl. Math.* **64** 225

Herman R L 1990a A direct approach to studying soliton perturbations *J. Phys. A: Math. Gen.* **23** 2321

Herman R L 1990b Conservation laws and the perturbed KdV equation *J. Phys. A: Math. Gen.* **23** 4719

Hof B, Juel A and Mullin T 2003 Scaling of the turbulence transition threshold in a pipe *Phys. Rev. Lett.* **91** 244502

Hof B, van Doorne C W H, Westerweel J, Nieuwstadt F T M, Faisst H, Eckhardt B, Wedin H, Kerswell R R and Wale F 2004 Experimental observation of nonlinear travelling waves in turbulent pipe flow *Science* **305** 1594

Itoh N 1977 Nonlinear stability of parallel flows with subcritical Reynolds numbers. Part 2. Stability of pipe Poiseuille flow to finite axisymmetric disturbances *J. Fluid Mech.* **82** 469

Leite R J 1959 An experimental investigation of the stability of Poiseuille flow *J. Fluid Mech.* **5** 81–96

Lou S Y, Tong B, Hu H and Tang X 2006 Coupled KdV equations derived from two-layer fluid *J. Phys. A: Math. Gen.* **39** 513

Lou S Y and Ni G J 1989 The relations among a special type of solutions in some $(D+1)$-dimensional nonlinear equations *J. Math. Phys.* **30** 1614

Mackrodt P A 1976 Stability of Hagen–Poiseuille flow with superimposed rigid rotation *J. Fluid Mech.* **73** 153–64

Mann E 1997a The perturbed Korteweg–de Vries equation considered anew *J. Math. Phys.* **38** 3772

Mann E 1997b Systematic perturbation theory for sine-Gordon solitons without use of inverse scattering methods *J. Phys. A: Math. Gen.* **30** 1227

Patera A T and Orszag S A 1981 Finite-amplitude stability of axisymmetric pipe flows *J. Fluid Mech.* **12** 467

Pringle C C T and Kerswell R R 2010 Using nonlinear transient growth to construct the minimal seed for shear flow turbulence *Phys. Rev. Lett.* **105** 154502

Rosenblat S and Davis S H 1979 Bifurcation from infinity *SIAM J. Appl. Math.* **37** 1

Ryzhov O S 2010 Solitons in transitional boundary layers *AIAA J.* **48** 275

Schneider T M, Eckhardt B and Yorke J A 2007 Turbulence transition and the edge of chaos in pipe flow *Phys. Rev. Lett.* **99** 034502

Schmid P J and Henningson D S 2001 *Stability and Transition in Shear Flows* (Berlin: Springer) p 556

Smith F T and Bodonyi R J 1982 Amplitude-dependent neutral modes in the Hagen–Poiseuille flow through a circular pipe *Proc. R. Soc.* A **384** 463–89

Smith F T, Doorly D J and Rothmayer A P 1990 On displacement-thickness, wall-layer and mid-flow scales in turbulent boundary layers and slugs of vorticity in channel and pipe flows *Proc. R. Soc.* A **428** 255–81

Waleffe F 1995a Transition in shear flows. Nonlinear normality versus non-normal linearity *Phys. Fluids* **7** 3060

Waleffe F 1995b Hydrodynamic stability and turbulence: beyond transients to a self-sustaining process *Stud. Appl. Maths.* **95** 319

Waleffe F 1997 On the self-sustaining process in shear flows *Phys. Fluids* **9** 883

Walton A G 2004 The stability of nonlinear neutral modes in Hagen–Poiseuille flow *Proc. R. Soc.* A **461** 813–24

Walton A G 2011 The stability of developing pipe flow at high Reynolds number and the existence of nonlinear neutral centre modes *J. Fluid Mech.* **684** 284–315

Wedin H and Kerswell R R 2004 Exact coherent structures in pipe flow: travelling wave solutions *J. Fluid Mech.* **508** 333

Willis A P and Kerswell R R 2009 Turbulent dynamics of pipe flow captured in a reduced model: puff relaminarisation and localised 'edge' states *J. Fluid Mech.* **619** 213

Willis A P, Peixinho J, Kerswell R R and Mullin T 2008 Experimental and theoretical progress in pipe flow transition *Phil. Trans. R. Soc.* A **366** 2671

Willis A P and Kerswell R R 2008 Coherent structures in localised and global pipe turbulence *Phys. Rev. Lett.* **100** 124501

Wygnanski I J and Champagne F H 1973 On transition in a pipe. Part 1. The origin of puffs and slugs and the flow in a turbulent slug *J. Fluid Mech.* **59** 281–335

Wygnanski I J, Sokolov M and Friedman D 1975 On transition in a pipe. Part 2. The equilibrium puff *J. Fluid Mech.* **69** 283–304

QUERY FORM

JOURNAL: fdr

AUTHOR: F Fedele

TITLE: Travelling waves in axisymmetric pipe flows

ARTICLE ID: fdr428608

Page 1

Q1.
Please verify the changes in the sentence ‘To leading order, ... nonlinearities’.

Page 2

Q2.
Please check the year with ‘Davey 1978’ in reference.

Page 18

Q3.
Please check the sentence ‘The convective ... less’ for clarity.

Page 20

Q4.
Please check the details for any journal references that do not have a blue link as they may contain some incorrect information. Pale purple links are used for references to arXiv e-prints.